RSC Advances

ROYAL SOCIETY OF CHEMISTRY

www.rsc.org/advances

The morphology of CuO adsorbent plays an important role in phosphine adsorption for purifying yellow phosphorus tail gas.

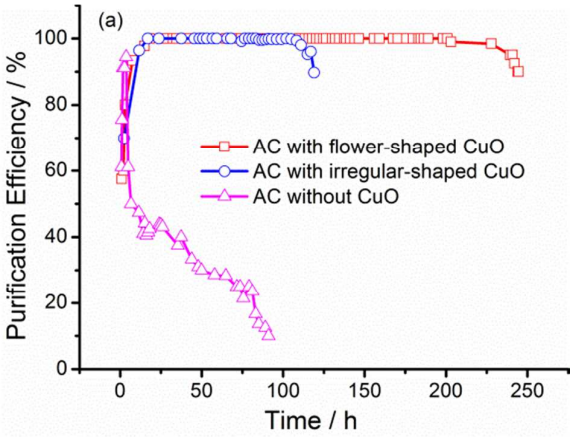

Purification process of Yellow Phosphorus Tail Gas for removal of PH_3 on the spot with flower-shaped CuO/AC

Zhandong Ren[1*], Shanshan Quan[1], Yuchan Zhu[1], Liang Chen[2], Wenxing Deng[1], Biao Zhang[1]

1.School of Chemistry and Environmental Engineering, Wuhan Polytechnic University, Wuhan 430023, P. R. China

2.Environmental Engineering & Science，Kunming University of Science and Technology，Kunming 650224, P. R.China

Abstract: The process of PH_3 adsorption removal for purifying yellow phosphorus tail gas on the spot with flower-shaped CuO was investigated in this study. The flower-shaped and irregular-shaped CuO/AC adsorbent were prepared by hydrothermal and impregnation method, respectively. They can effectively remove PH_3 less than 1 $mg \cdot m^{-3}$ and the purification efficiency is nearly 100% without fluctuation. However the morphology of CuO on the adsorbent surface plays an important role in phosphine adsorption. The breakthrough adsorption capacity of flower-shaped CuO adsorbent was 96.08 mg(PH3)/ g(adsorbent), which was nearly twice for irregular-shaped CuO. The purification efficiency of flower-shaped CuO was also influenced by temperature, oxygen volume fraction and space velocity. Under the situation of temperature 100 ℃ and oxygen volume fraction 1.6%, the adsorption capacity is the best. The adsorbent can be renewed and the regenerated catalyst can also efficiently remove PH_3 which the purification efficiency is nearly 100%. In the process of catalytic oxidation, according to XPS, we can conclude that CuO plays a very important role in phosphine adsorption and oxygen is able to accelerate the PH_3 oxidation and oxidize Cu to regenerate the active species in the process of purification.

Key words： yellow phosphorus tail gas; PH_3; flower-shaped CuO; morphology; on the spot

---

* Corresponding author. E-mail: renzhandong@163.com

1. Introduction

Yellow phosphorus is an important chemical product. There is about 2500-3000Nm^3 byproduct, tail gas, when producing 1t yellow phosphorus[1]. The concentration of CO is above 85% (vol ratio) and caloric value is about 11700 $kJ \cdot m^{-3}$ in tail gas[2]. At present, most yellow phosphorus manufacturers just use tail gas as fuel or directly discharge it through torch burning. The burned gases with greenhouse gas CO_2 (include phosphate, sulfide and fluoride etc.) are given off into atmosphere and cause great environmental pollution. At the same time, it is also a great waste of CO gas.

The contents of different ingredients in tail gas varied with different processing techniques in phosphor producing, and the typical contents of yellow phosphorus tail gas is showed as follows[3-5]. It mainly consists of CO(85~90 vol%) and other contents such as CO_2(2~4 vol%), N_2(3~5 vol%), H_2(3~5 vol%), CH_4(0.4 vol%), O_2(0.2 vol%), H_2S(600~3000 $mg \cdot m^{-3}$), COS(20~2000 $mg \cdot m^{-3}$), CS_2(1~50 $mg \cdot m^{-3}$), P_4 and PH_3(500~1000 $mg \cdot m^{-3}$), HF and SiF_4(400~500 $mg \cdot m^{-3}$) and AsH_3(1~8 $mg \cdot m^{-3}$) etc. PH_3 is a potent catalyst poison in CO synthesizing chemistry even at a low concentration[6, 7]. Moreover, considering its high toxicity and carbon monoxide (CO) resources waste, PH_3 removal from yellow phosphorus tail gas has become a compelling issue. After removing completely (less than 5 $mg \cdot m^{-3}$)[6, 7], yellow phosphorus tail gas can be used as chemical resource to produce chemical products, such as methanol, methyl formate, dimethyl oxalate, dimethyl carbonate and dimethyl ether etc[8-12].

During the past several decades, most researches were focus on removing PH_3 by absorption method. The activated carbon can absorb PH_3[2, 13], but the maximum adsorption capacity was only 12 mg-PH_3/ g-activated carbon (AC) and cannot reduce the PH_3 content less than 5 $mg \cdot m^{-3}$. Based on the literature[14-21], catalytic oxidation method with metal oxide catalysts was adopted to remove PH_3 gas in the literature. The method is simple, convenient operation, economical investment and high efficient removal of phosphors. Copper oxide is commonly used as the active species. Li[22] had inspected Cu/ZSM-5(Y) zeolite adsorbents and the maximum adsorption

capacity was 31 mg-PH_3/g-adsorbent. Chang[23]had prepared a novel sol-gel-derived Cu/TiO_2 adsorbent which had been demonstrated to exhibit exceptional capacities of 40.62, 49.52, and 108.48 mgPH_3/ gCu/TiO_2 for the oxidative capture of phosphine (PH_3) in N_2, air, and humidified air, respectively. Yu[1] had studied Cu/AC absorbents which were prepared by various copper precursors, impregnation solution concentration, and calcination temperature. The biggest PH_3 breakthrough adsorbed amount was 112.38 mg-PH_3/g-adsorbents. Yang[24], Ning[25] and Yi[20] had prepared a series of Cu/AC with Zn, Ce, Zn, Fe, La, Ce to further improve the purify efficiency on PH_3 adsorption removal.

However, the morphology of absorbent on the PH_3 adsorption performance has never been studied. In the gas desulfurizerization, some researchers[26] had investigated the importance of morphology. Jung[27] found that absorbents with different surface area, make a significant difference in desulfurization performance, and they suggested that surface area contribute to the capacity of the sorbent. So we think that the investigation of the morphology influence of absorbents on dephophorization is thus quite important and very necessary. In addition, in many literatures, PH_3 was removed of the mixed simulation gas (PH_3+N_2), not the actual yellow phosphorus tail gas (PH_3+CO) on the scene. There is a vast difference between the two in the carrier gas, one of which is an inert atmosphere; the other is a reducing atmosphere. In the process of purification, phosphine adsorbed on the activated carbon would be oxidized to form P_2O_3 or P_2O_5 by oxygen and these oxidization products could be adsorbed onto activated carbon more easily than PH_3. But the oxygen also can react with CO to form CO_2, thus affecting the phosphine oxide adsorption. So the objective of this research was to study the morphology of CuO/AC absorbents and the purification process parameters in situ for PH_3 removal in the yellow phosphorus tail gas. This is beneficial to industrial application.

2. Materials and methods

2.1 The preparation and regeneration of adsorbent

The active carbon(AC) purchased from a commercial carbon (Sinopharm

Chemical Reagent Co., Ltd., Shanghai, China) was used as adsorbent support in this study. First, the AC support was crushed and sieved to 1-2 mm, followed by washing with distilled water, filtration, and dried at 120 ℃ for 3h. The irregular-shaped CuO/AC adsorbents were prepared by the impregnation of 2 g pretreated AC with an aqueous solution of 0.2 $mol \cdot L^{-1}$ $Cu(NO_3)_2$ (30 ml). Then the impregnation was carried out under stirring for 24 h. These wet samples were dried in a drying cabinet at 120 ℃ for 3 h followed by calcining in a furnace at a calcination temperature at 400 ℃ for 2 h (heating rate 5 ℃/min). The flower-shaped CuO/AC adsorbents were prepared by hydrothermal method. Sodium citrate (2 g) and active carbon (2 g) were added to 0.2 $mol \cdot L^{-1}$ $CuCl_2 \cdot 2H_2O$ (30 ml) under vigorous stirring. Precipitation was done by dropwise addition of 7.5 $mol \cdot L^{-1}$ Sodium hydroxide (2 ml). The obtained suspension was added to the autoclave at 180 ℃ for 6 h. Then the precipitate was filtered, thoroughly washed with water, and oven dried overnight at 120 ℃. The absorbent regeneration experiments were carried out on the catalyst which had failed after purifying tail gas for 250 h. The deactivated CuO/AC catalyst was dealt in place with air oxidation, water vapor washing, alkaline washing, water washing and drying in the adsorption tower to regenerate.

2.2 Material characterization

X-ray diffraction (XRD) were used to analyze the structures of the flower-shaped and irregular-shaped CuO. The inspection was carried out at room temperature on a D/Max-ⅢA diffractometer (Rigaku, Japan), using Cu K_α radiation operating at 40 kV and 30 mA. The surface morphology was characterized by scanning electron microscopy (SEM: S-3000N, Hitachi Co., Japan). The analysis of the composition was characterized by X-ray Fluorescence (XRF: EDX-720, Shimadzu, Japan). Micromeritics ASAP2020 surface area analyzer was used to measure N_2 adsorption isotherms at -196 ℃. The BET surface area was calculated from the isotherms using the Brunauer–Emmett–Teller (BET) equation.

2.3 Adsorption purification process

The tail gas was come from the yellow phosphorus production workshop of Yunnan Jianglin Group Phosphide-product Company and the gas composition was close to the typical contents of yellow phosphorus tail gas as mentioned above. Before coming into the gas adsorption tower, the majority of hydrogen sulfide in yellow phosphorus tail gas was removed through alkaline washing. The tail gas with the PH_3 content of 300~1000 $mg \cdot m^{-3}$ was sent into the gas adsorption tower. The adsorption tower is designed with the inner diameter of 5 cm and the height of 50 cm (Fig. 1). Evaluations of adsorbents for dephosphorization were conducted in a upflow fixed-bed with 25.5 cm bed height at atmosphere pressure, 40~110 °C, and space velocity of 750-1300 h^{-1}, using a tail gas (>90% CO and 0.5-2.0% O_2). The tail gas is analyzed from sampling port at the top of the tower. In this experiment, the contents of PH_3 in both the raw material gas and purification gas are analyzed by PH_3 content detecting-tube (made by Beijing labor and protection institute technological developing company).

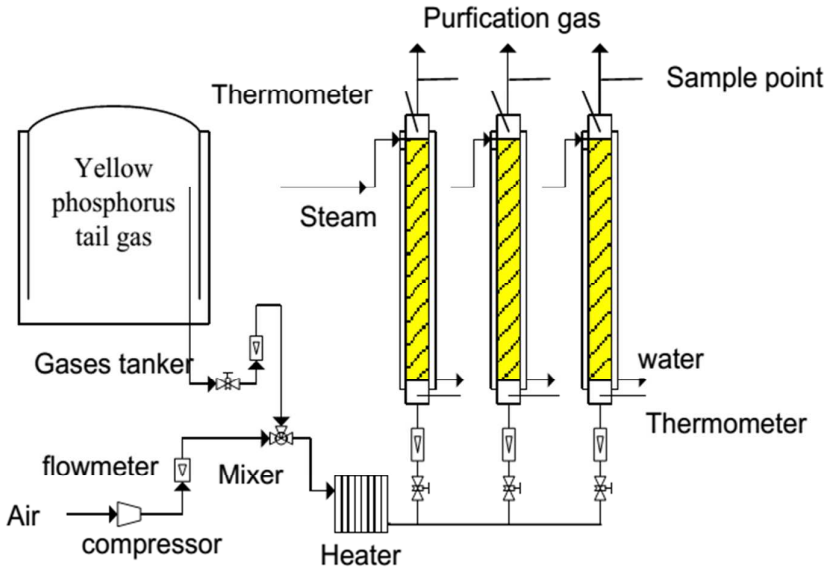

Fig.1 Schematic diagram of the purification process

2.4 Purification efficiency and adsorption capacity

The tail gas purification efficiency is defined as the efficiency that the harmful impurities has been purified in tail gas. It can be expressed by the following formula:

$$f = \frac{c_0 - c_f}{c_0} \times 100\%$$

f: Purification efficiency

c_0: PH_3 content in yellow phosphorus tail gas, $mg \cdot m^{-3}$

c_f: PH_3 content after purified, $mg \cdot m^{-3}$

Dephosphorization of the asorbent was continued until the breakthrough point. The breakthrough point was defined as the PH_3 content exceeding 5 $mg \cdot m^{-3}$ of the outlet gas. The adsorption capacity can be expressed by the following formula:

$$\Gamma = \frac{V \times GHSV \times t \times c}{m}$$

Γ: Adsorption capacity, $mg(PH_3)/g(absorbent)$

V: Bed volume, m^3

$GHSV$: Gas hourly space velocity, h^{-1}

t: Time, h

c: PH_3 content, c_0-c_f, $mg \cdot m^{-3}$

m: The weight of absorbent, g

3. Results and discussions

3.1 Crystal structure and morphology

The morphology of as-prepared CuO with hydrothermal and impregnation method were observed with FESEM. In Fig. 2, the black areas with big particles in background are the active carbon carriers and the bright areas are CuO particles. The clear view of flower-shaped structure using hydrothermal method was seen in Fig. 2(a). The leafy nanosheets reveal that the flowers are consists of many tiny petals in Fig. 2(b). The typical length of one petal is about 300-500 nm, while the diameter is in the range of 200-300 nm. The full array of one flower-shaped structure with circumferential symmetry is in the range of 800-1000 nm. The CuO with simple impregnation and calcination method were irregular-shaped particles in Fig.2(c). Comparison of Fig. 2(a) and Fig. 2(c), we can conclude that the flower-shaped structure would provide more surfaces and active sites for the reaction. It can also be

proved from the characterization of BET, which the specific surface area of flower-shaped and irregular-shaped CuO was 38.15 $m^2 \cdot g^{-1}$ and 25.03 $m^2 \cdot g^{-1}$, respectively.

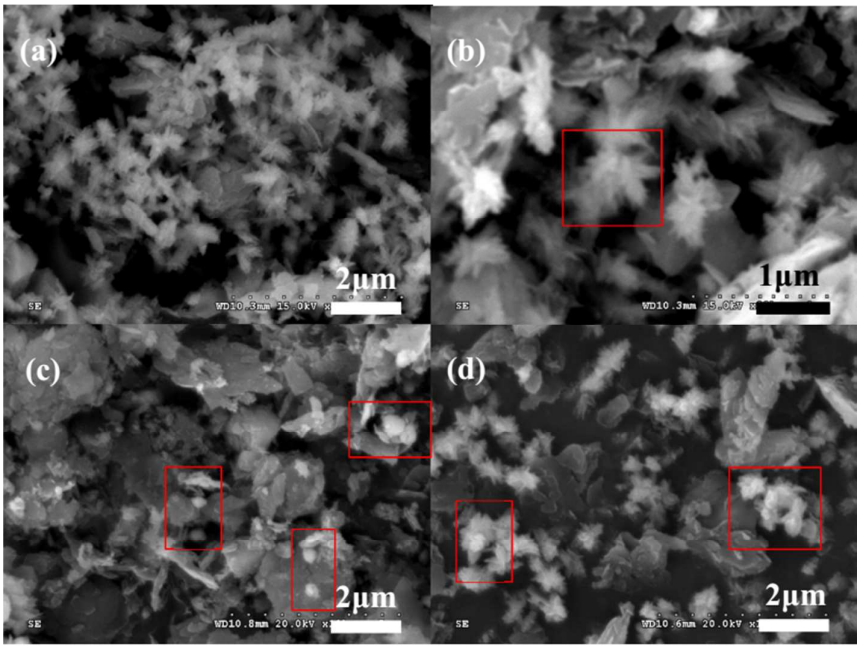

Fig. 2 SEM images of CuO nanostructures with flower-shape (a, b) and irregular-shape (c) and regenerated flower-shaped CuO (d)

The crystallinity and crystal phases of the flower-shaped and irregular-shaped CuO were examined by the X-ray diffraction pattern and shown in Fig. 3. All the reflection on the XRD pattern could be indexed to the monoclinic CuO phase with lattice constants comparable to the reported date (JCPDS 05-0661). Moreover, the major peaks located at 2θ values of 35.6^O and 38.8^O indexed as $(\bar{1}11)$ and (111) planes, respectively, are characteristics for the CuO crystallites. In Fig. 3, there are extra two diffraction peaks located at 2θ values of 36.4^O and 42.2^O indexed as (111) and (200) planes of Cu_2O crystal in the irregular-shaped CuO sample, which is due to a small amount of copper was not completely oxidized in the process of the thermal oxidation preparation. The Cu_2O has poor adsorption performance of PH_3[18, 21], so it would reduce its adsorption performance. But no other peaks related to other phases and impurities were not found in the XRD pattern of the flower-shaped CuO,

which were attributed to the hydrothermal preparation process. In addition, the diffraction peak intensity of irregular-shaped CuO is stronger than that of flower-shaped CuO, which may be due to the high sintering temperature in the impregnation preparation process. The nominal CuO loading is 19.35wt% and the actual content loading which was measured by XRF is 16.10wt% for flower-shaped CuO and 17.42wt% for irregular-shaped CuO, respectively.

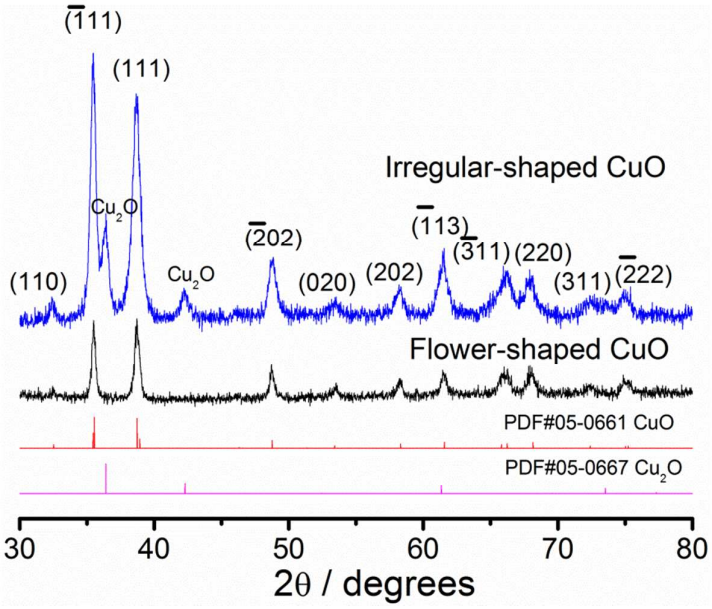

Fig. 3 XRD pattern of flower-shaped and irregular-shaped CuO

3.2 Effect of the morphology of CuO for PH_3 adsorption removal

As shown in Fig. 4(a), the AC adsorbent without CuO loading showed very poor PH_3 adsorption capacity. According to the phosphine removal efficiency curve, the purification efficiency was below 50% after the initial 10 h and the PH_3 adsorption capacity was only 1.50 mg(PH_3)/g(adsorbent). However, the PH_3 removal efficiency was significantly enhanced through CuO loading, in particularly flower-shaped CuO. At the early stage, the adsorbents were gradually activated and the PH_3 purification efficiency had gradually increased to 100% after 15 h. At the stable stage, the purification efficiency was almost fixed in 100% without fluctuation, which shows that CuO/AC catalyst has good activity to remove PH_3. The adsorption capacity of flower-shaped CuO adsorbent is 96.08 mg(PH_3)/g(adsorbent), which is 2.23 times

for irregular-shaped CuO. That is partly because the BET specific surface area of flower-shaped CuO is larger than irregular-shaped CuO. On the other hand, the morphology of absorbent would have a great meaning in its performance. So the comparative calculation of adsorption capacity in respect to overall BET would clarify the differences between both catalysts. In Fig. 4(b), in the unit surface area, the adsorption capacity of flower-shaped and irregular-shaped CuO adsorbent is 2.52 and 1.72 mg(PH_3)/m^2(adsorbent) respectively. Therefore, the morphology of CuO on the adsorbent surface also play an important role in phosphine adsorption. In addition, from the X-ray diffraction pattern, there is a small amount of Cu_2O crystal in the irregular-shaped CuO adsorbent, which is also the reason for the poor adsorption performance.

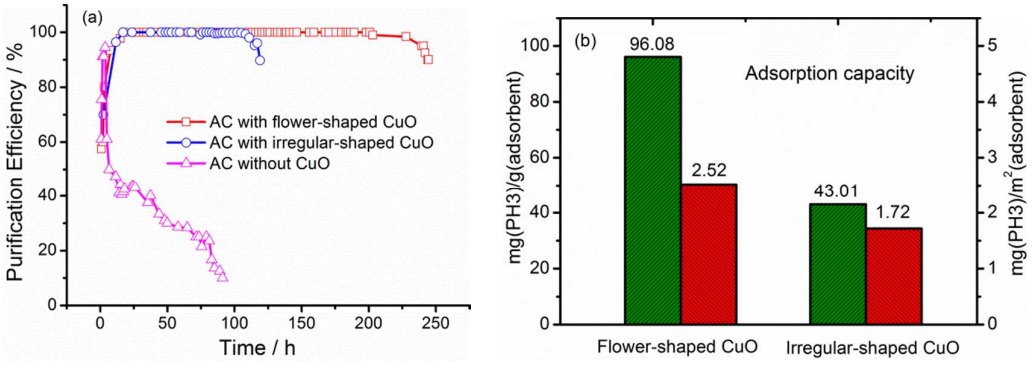

Fig. 4 PH_3 removal efficiency curves of flower-shaped, irregular-shaped CuO/AC and AC adsorbents. Experimental conditions: Load capacity=19.35%, Bed height=25.5 cm, T=110 ℃, [PH_3]=350 mg·cm^{-3}, [O_2]=1.6%, and GHSV=750 h^{-1}.

3.3 Effect of oxygen content for PH_3 adsorption removal

Fig. 5 illustrates the effect of the oxygen concentration on the performance of PH_3 purification. Oxygen content is one of the most important factors, which influences the PH_3 adsorption capacity. Direct oxidation of PH_3 with gaseous O_2 is inefficient at room temperature. However, adsorbed O_2 molecules are able to accelerate the PH_3 oxidation and also oxidize the reduced Cu^0 metals and Cu^+ ions to regenerate the active species for further PH_3 capture. As observed in Fig. 5(a), in the absence of O_2, the breakthrough of PH_3 occurs in approximately 36 h and the adsorption capacities

is only 18.70 mg(PH_3)/g(adsorbent). Once 0.5 vol% oxygen was introduced into tail gas, the breakthrough time was increased to 144 h and the adsorption capacities was improved significantly to 74.79 mg(PH_3)/g(adsorbent). When the volume fraction of oxygen had risen to 1.2% and 1.6%, the adsorption capacities were further expanded to 87.25 and 99.72 mg(PH_3)/g(adsorbent).

In Fig. 5(b), the influence of the oxygen concentration was further discussed in detail. When the oxygen volume fraction was 0.5 vol% and purification time was 192 h, the purification efficiency was 94.29% and the mass fraction of PH_3 was 20 $mg \cdot m^{-3}$. With the gradual increase of the volume fraction of oxygen, the purifying efficiency had improved significantly. When the oxygen contents were 0.9%, 1.2%, and 1.6%, the mass fraction of PH_3 and purification efficiency were 16 $mg \cdot m^{-3}$, 6 $mg \cdot m^{-3}$, 1 $mg \cdot m^{-3}$ and 95.43%, 98.29%, 99.71%, respectively. If the volume fraction of oxygen further enhanced, the purification efficiency was stable at nearly 100%. But too much oxygen would make CO oxidize into CO_2 and bring the excessive residual oxygen in the exhaust gas. It would make the follow-up processing difficult to deal with and bring some security problems, so the optimum oxygen volume fraction is 1.6%. In addition, when the oxygen volume fraction was 1.6%, the purification efficiency was still nearly 100% with the increase of PH_3 content from 350 $mg \cdot m^{-3}$ to 900 $mg \cdot m^{-3}$ in the exhaust gas (see table S1).

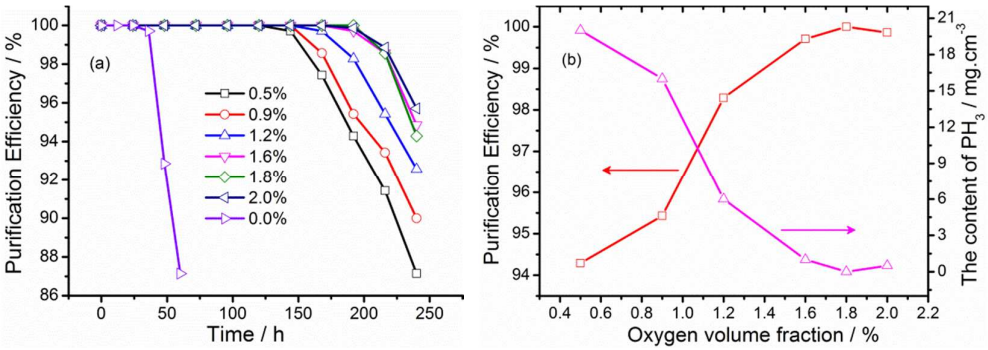

Fig. 5 The effect of oxygen volume fraction on the PH_3 purification with flower-shaped CuO/AC. Experimental conditions: Adsorbent = flower-shaped CuO, Load capacity=19.35%, Bed height=25.5 cm, T=110 ℃, [PH_3]=350 $mg \cdot cm^{-3}$, and GHSV=750 h^{-1}.

3.4 Effect of adsorption temperature for PH_3 adsorption removal

In the adsorption process, the reaction temperature has great influence on the PH_3 purification efficiency of yellow phosphorous tail gas (Fig. 6). When the reaction temperature was 40 ℃, the purification efficiency was 98.33% and the content of PH_3 in the purified gas was 15 $mg \cdot m^{-3}$. It cannot be used as a raw material gas to produce C1 chemical products, such as ethanol, methyl formate, dimethyl oxalate, dimethyl carbonate and dimethyl ether etc[8-12]. Because trace phosphine (more than 5 $mg \cdot m^{-3}$) could cause carbonylation catalysts poisoning and expiration[6, 7]. With the increase of adsorption temperature, the content of PH_3 decreased and purification efficiency enhanced. When the adsorption temperature was 100 ℃, the purification efficiency was 100% and the content of PH_3 in the purified gas was reduced to 0 $mg \cdot m^{-3}$. If the temperature rises to 120 ℃and 140 ℃, the PH_3 content of purified tail gas was still less than 1 $mg \cdot m^{-3}$.

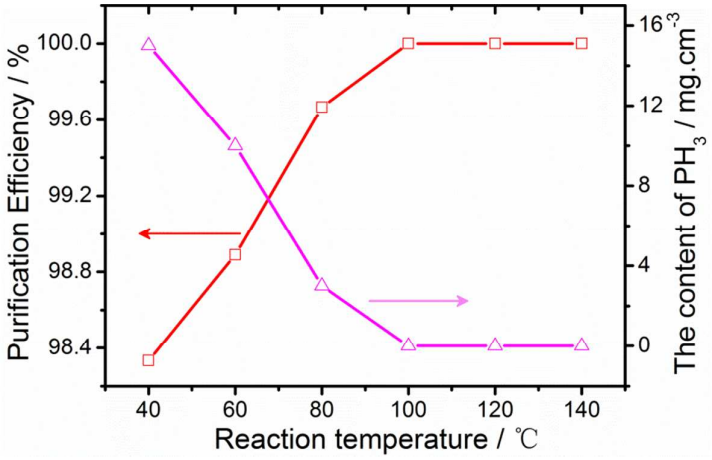

Fig. 6 The effect of adsorption temperature on the PH_3 purification with flower-shaped CuO/AC. Experimental conditions: Adsorbent = flower-shaped CuO, Load capacity=19.35%, Bed height=25.5 cm, $[PH_3]$=900 $mg \cdot cm^{-3}$, $[O_2]$=1.6%, and GHSV=750 h^{-1}.

3.5 Effect of space velocity for Adsorption capacity of PH_3

The PH_3 purification efficiency curves with different amount of tail gas to be treated are presented in Fig. 7. When the GHSV was grown from 750 h^{-1} to 1100 h^{-1}, 1300 h^{-1} respectively, the PH_3 purification efficiency was still remained at 100%. But

the available purification time had reduced to 123 h and 108 h, which was 186 h for 750 h^{-1}. This may be explained by considering that with the GHSV increasing, the amount of processing is also raised in unit time, resulting in the reduction of the available purification time of tail gas. However, their adsorption capacities were nearly the same, 96.08, 93.28 and 94.50 mg(PH_3)/ g(adsorbent) respectively.

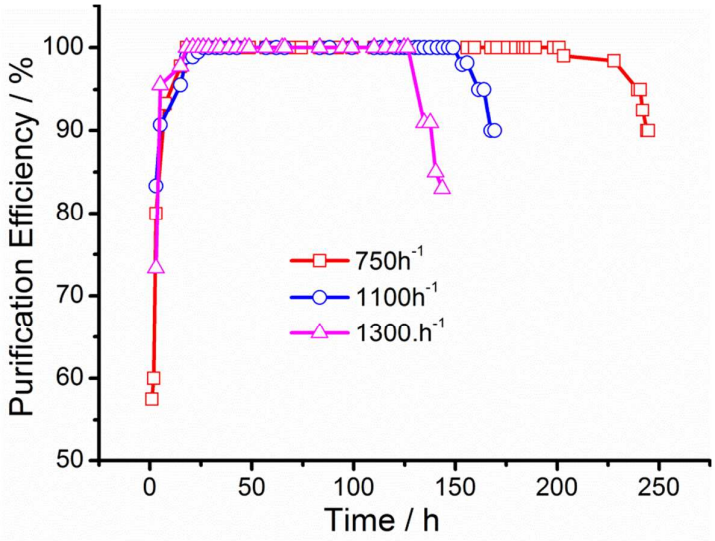

Fig. 7 PH_3 purification efficiency curves with different GHSV. Experimental conditions: Adsorbent = flower-shaped CuO, Load capacity=19.35%, Bed height=25.5 cm, [PH_3]=350 mg·cm^{-3}, [O_2]=1.6%, and T=110 ℃.

3.6 Catalyst regeneration

It is very important for catalyst to regenerate in the industrial production. Cyclic use of catalyst can reduce the production cost and increase its utilization value. So the regeneration experiments were carried out on the catalyst which had failed after 250 h purification. From the purification curve after regeneration (Fig. 8), it was seen that the regenerated catalyst can remove PH_3 efficiently. The purification efficiency had reached 100% which is the same as the fresh catalyst. The regeneration result of CuO adsorbent indicates that the majority of phosphorus has been successfully taken place through air oxidation, water vapor washing, alkaline washing, water washing and drying. But the regenerated catalyst's stability was not good enough, especially after 100 h purification, the trace amounts of PH_3 (less than

5 mg·m^{-3}) could sometimes be detected in the purified gas. In order to analyze the reason of the decreased activity, SEM characterization of regenerated CuO was made. As shown in the Fig. 2(a) and 2(d), the amount of crystal particles of the regenerated CuO was less than the fresh CuO. It is perhaps due to the loss of copper in the process of regeneration and the uneven dispersion of CuO particles on the activated carbon. However, the regenerated CuO still remains the morphology of flower-structure, which was prepared by hydrothermal method under high temperature and high pressure. Unfortunately, it was seemed to observe that some crystal particles had covered on the surface of CuO, which had been marked with a red box in the SEM image. This is probably the phosphorus oxide generated in the process of purification, which was not removed thoroughly during regeneration. It would reduce the specific surface area, thus decrease the adsorption efficiency and adsorption capacity. In addition, in the regeneration process, Cu^0 and Cu^+ were perhaps not fully oxidized into Cu^{2+}, so the capacity is primarily limited by the incompletely oxidized intermediates.

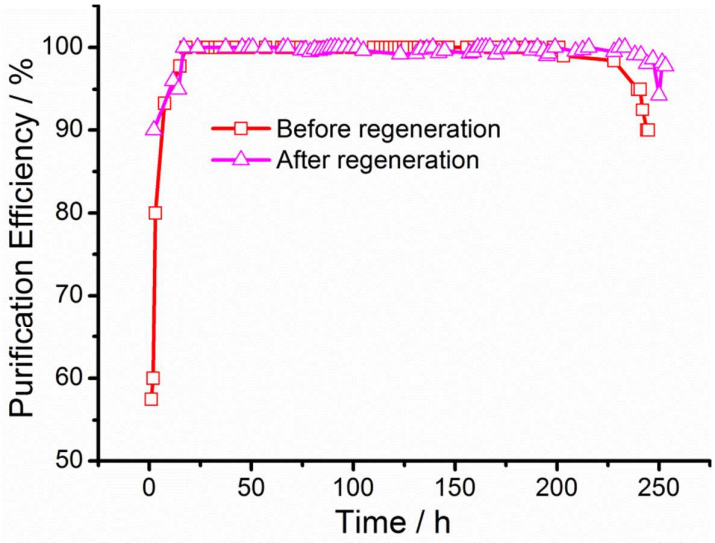

Fig. 8 The purification curve of the regenerated catalyst with flower-shaped CuO/AC. Experimental conditions: Load capacity=19.35%, Bed height=25.5 cm, T=110℃, [PH_3]=350 mg·cm^{-3}, [O_2]=1.6%, and GHSV=750 h^{-1}.

3.7 Oxidation and adsorption process

During the adsorption process, direct oxidation of PH_3 with gaseous O_2 is inefficient. However, catalytic oxidation reaction can take place under the existing of CuO. PH_3 can be oxidized into P_2O_3 and P_2O_5 and the adsorptive capacity for P_2O_3 and P_2O_5 is far more than that for PH_3. The mechanisms associated with oxidation process are summarized as follows:

$$2PH_3 + 3O_2 \xrightarrow{CuO} P_2O_3 + 3H_2O$$

$$2PH_3 + 4O_2 \xrightarrow{CuO} P_2O_5 + 3H_2O$$

Moreover PH_3 is chemisorbed on one of the embedded CuO moieties through P-Cu chelating and can be oxidized into H_3PO_4, which can be easily absorbed on the active carbon. The process is as follow:

$$PH_3 + 2O_2 \xrightarrow{CuO} H_3P\ O_4$$

Chang[21] had put forward the catalytic mechanism.

$$PH_3 \rightarrow PH_2 \rightarrow H_2P - OH \rightarrow HP(OH)_2 \rightarrow P(OH)_3 \rightarrow HO - P = O \rightarrow H_3PO_4$$

H^+ ion is dissociated from the PH_3 to protonate the O^{2-} ion. The chemisorbed PH_2 then donates 2 electrons to reduce the bonded Cu^{2+} into Cu^0 while oxidizing itself via hydroxylation to form a $P(OH)H_2$ species. The $P(OH)H_2$ intermediate follows a similar dissociative chemisorption to react with the next CuO until the PH_3 becomes $P(OH)_3$ and H_3PO_4.

To clarify the reaction between the CuO and the PH_3, we analyzed the chemical states and chemical environments of the Cu and P species using XPS. Fig. 9(a) shows the Cu 2p XP spectra of the CuO both before and after the capture of PH_3. Before adsorption, the Cu $2p_{3/2}$ peak centered at 933.42 eV and 935.56 eV can be assigned to CuO and $Cu(OH)_2$. The as-prepared CuO sample contained two satellite peaks at the binding energy (BE) of 944.4 eV and 963.6 eV, clearly indicating Cu 2p ions. After the capture of PH_3, the Cu $2p_{3/2}$ peak shifted to 932.66 eV. This indicates that the Cu exists with a chemical state other than the CuO form, which is Cu_2O or Cu. The change of peak intensity about the CuO adsorbents before and after adsorption is due to the phosphorus deposition that results from the adsorption and

subsequent oxidation of phosphine on the CuO adsorbent. In addition, the satellite peaks disappearing also indicate Cu species was reduced. Fig. 9(b) shows the P 2p XP spectra of the CuO sample after the capture of PH_3. According to the literature[23], it could ascribe the 130.3, 132.8, and 133.7 eV to P, P^{3+}(P_2O_3), and P^{5+}(P_2O_5 and H_3PO_4) states, respectively, because they stayed either in a stable closed shell and or in a half-filled configuration. Fresh adsorbent has no phosphorus species, so the P_2O_3, P_2O_5 or H_3PO_4 species appearing in the exhausted sample were generated by an oxidation process. According to the above catalytic mechanism, we can conclude that CuO plays a very important role in phosphine adsorption and oxygen is able to accelerate the PH_3 oxidation and oxidize Cu to regenerate the active species in the process of purification.

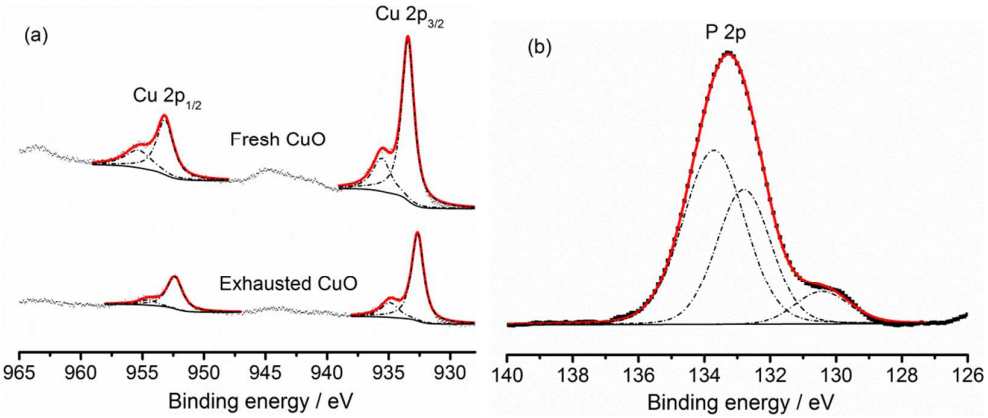

Fig. 9 XPS spectra of Cu 2p with the fresh CuO adsorbent and the exhausted CuO adsorbent (a) and P 2p with the exhausted CuO adsorbent (b). The experimental results, the fitted peaks, and the summarized results of the fitted data are presented as dotted, dashed, and solid curves, respectively.

4. Conclusions

The process of PH_3 adsorption removal for purifying yellow phosphorus tail gas on the spot was investigated in this study. The morphology of CuO on the adsorbent surface plays an important role in phosphine adsorption. The flower-shaped CuO/AC adsorbent can effectively remove PH_3 less than 1 $mg \cdot m^{-3}$ without fluctuation and adsorption capacity is 96.08 mg(PH3)/g(adsorbent), which is nearly twice for

irregular-shaped CuO. The purification efficiency was also influenced by oxygen volume fraction. Oxygen is able to accelerate the PH_3 oxidation and oxidize Cu to regenerate the active species in the process of purification. When the adsorption temperature was above 100 ℃, the purification efficiency was 100% and the content of PH_3 in the purified gas was reduced to 0 $mg \cdot m^{-3}$. The adsorbent can be renewed and the regenerated catalyst can also efficiently remove PH_3 which the purification efficiency is nearly 100%. During the catalytic oxidation adsorption process, PH_3 can be oxidized into P_2O_3 or P_2O_5 and CuO plays a very important role in phosphine adsorption and oxidation.

Acknowledgements

This work was supported by the Natural Science Foundation of Hubei Province (2012FFB04803) and the National Natural Science Foundation of China (31101370).

References

[1] Q. F. Yu, P. Ning, H. H. Yi, X. L. Tang, M. Li and L. P. Yang, *Sep. Sci. Technol.*, 2012, **47**, 527–533.

[2] L. P. Ma, P. Ning, Y. Y. Zhang and X. Q. Wang, *Chem. Eng. J.*, 2008, **137**, 471-479.

[3] P. Ning and B. N. Ren, *Yunnan Environ. Sci.*, 2003, **22**, 149~151.

[4] H. P. Gao, P. Ning, C. F. Wu and M. X. Ma, *Journal of Wuhan University of Technology-Mater. Sci. Ed.*, 2010, **2**, 53-57

[5] Z. H. Wang, M. Jiang, P. Ning and G. Xie, *Ind. Eng. Chem. Res.*, 2011, **50**, 12194–12202

[6] X. Q. Wang, P. Ning, Y. Shi and M. Jiang, *J Hazard. Mater.*, 2009, **171,** 588-593.

[7] R. Quinn, T. A. Dahl, B. W. Diamond and B. A. Toseland, *Ind. Eng. Chem. Res.*, 2006, **45**: 6272-6278.

[8] C. J. Yoo, D. W. Lee, M. S. Kim, D. J. Moon and K. Y. Lee, *J. Mol. Catal. A-Chem.*, 2013, **378,** 255-262.

[9] S. Goodarznia and K. J. Smith, *J. Mol. Catal. A-Chem.*, 2012, **353-354**, 58-66.

[10] Z. N. Xu, J. Sun, C. S. Lin, X. M. Jiang, Q. S. Chen, S. Y. Peng, M. S. Wang and G. C. Guo, *ACS. Catal.*, 2013, **3,** 118-122.

[11] J. Q. Wang, J. Sun, C. Y. Shi, W. G. Cheng, X. P. Zhang and S. J. Zhang, *Green Chem.*, 2011, **13:** 3213-3217.

[12] K. G. Mbuyi, M. S. Scurrell, D. Hildebrandt and D. Glasser, *Top Catal.*, 2012, **55**: 1261-1268.

[13] Q. F. Yu, M. Li, P. Ning, H. H. Yi and X. L. Tang, *Sep. Sci. Technol.* 2014, **49**: 2366–2375.

[14] D. He, H. H. Yi, X. L. Tang, P. Ning, K. Li, H. Y. Wang and S. Z. Zhao, *J. Mol. Catal. A-Chem.*, 2012, **357,** 44-49.

[15] Y. C. Liu and H. He, *J. Phys. Chem. A*, 2009, **113**: 3387-3394.

[16] P. Ning, K. Li, H. H. Yi, X. L. Tang, J. H. Peng, D. He, H. Y. Wang and S. Z. Zhao, *J. Phys. Chem. C*, 2012, **116**, 17055-17062.

[17] L. Wang, S. D. Wang and Q. Yuan, *Fuel Process Technol.*, 2010, **91**, 777-782.

[18] X. Q. Wang, J. Qiu, P. Ning, X. G. Ren, Z. Y. Li, Z. F. Yin, W. Chen and W. Liu, *J. Hazard. Mater.*, 2012, **229-230**, 128-136.

[19] H. H. Yi, D. He, X. L. Tang, H. Y. Wang, S. Z. Zhao and K. Li, *Fuel*, 2012, **97**, 337–343.

[20] H. H. Yi, Q. F. Yu, X. L. Tang, P. Ning, L. P. Yang, Z. Q. Ye and J. H. Song, *Ind. Eng. Chem. Res.*, 2011, **50**, 3960–3965.

[21] H. H. Yi, S. Z. Zhao, X. L. Tang, P. Ning, H. Y. Wang and D. He, *Catal. Commun.*, 2011, **12**, 1492-1495.

[22] W. C. Li,; H. L. Bai, J. N. Hsu, S. N. Li and C. C. Chen, *Ind. Eng. Chem. Res.*, **2008**, 47, 1501-1505.

[23] S. M. Chang, Y. Y. Hsu and T. S. Chan, *J. Phys. Chem. C*, 2011, **115**, 2005–2013.

[24] L. P. Yang, H. H. Yi, X. L. Tang, P. Ning, Q. F. Yu and Z. Q. Ye, *J. Rare Earths*, 2010, **28**, 322-325.

[25] P. Ning, H. H. Yi, Q. F. Yu, X. L. Tang, L. P. Yang and Z. Q. Ye, *J. Rare Earths*, 2010, 28, 581-586.

[26] M. Pineda, J. M. Palacios, F. Tomas, C. Cilleruelo, E. Garcia and J. V. Ibarra, *Energy Fuels*, 1998, **12**, 409−415.

[27] S. Y. Jung, H. K. Jun, S. J. Lee, T. J. Lee, C. K. Ryu and J. C. Kim, *Environ. Sci. Technol.*, 2005, **39**, 9324−9330.